DESIGN AND MAGNETIC MEASUREMENT OF THE NAL MAIN ACCELERATOR BENDING MAGNETS

R. Yamada, C. Schmidt, R. Juhala
National Accelerator Laboratory*, Batavia, Illinois

and R. Lari
Argonne National Laboratory, Argonne, Illinois

Abstract

Profiles of the NAL Main Ring Bending Magnets were calculated by the computer program TRIM. The calculated field gradient k = (dB/dx)/B_o is compared with the measured values. The effect of insulation thickness, shims, and imperfection of the dies are discussed. The selection criteria for the Main Ring Magnet steel are presented. The test procedures used for determining the coercive force, high field μ-value, surface resistivity and crown are described. The variation of these parameters during steel production are presented and the effect on the magnets discussed. Production magnetic field test procedures and the results are described. Data on the variations in magnetic length are presented for B1 and B2 magnets.

Introduction

In the main ring there are 378 B1 bending magnets (1.5 x 5 in. aperture), 396 B2 bending magnets (2 x 4 in. aperture), and 240 quadrupole magnets (including the 7 and 4 foot magnets).[1] There are about 50 B1 and 50 B2 bending magnets and about 20 quadrupole magnets which are designated as spare magnets or for use in the experimental beam line. Early conceptual designs of these magnets were reported in a number of papers.[1,2,3,4] The results of the magnetic measurements on early model magnets were reported as NAL internal reports.[5,6,7,8] A preliminary test on the steel evaluation is also given in an internal report.[9]

The mechanical design of the main ring magnets is published in other papers[10,11] and the results of measurements made on the final design were briefly given at the 1971 Particle Accelerator Conference.[12,13] It is the intent of this paper to supplement the previous papers by giving the details of the final design of the pole faces, the results of the field measurements, the production test results of the bending magnets, and the characteristics of the production steel.

*Operated by Universities Research Association, Inc. under contract with the United States Atomic Energy Commission.

Computer Calculation of the Bending Magnets

The cross sections of the B1 and B2 bending magnets were determined by calculating the field uniformity using the computer program TRIM.[14] This was done on the IBM S/360 model 50/75 at Argonne National Laboratory. The program is designed to take advantage of magnet symmetry and thereby economize on computer time. In this case, one-fourth of the magnet cross section (7.125 in. high by 12.625 in. wide) is sufficient to determine the field. A total of 4950 mesh points were used and distributed in such a manner that a mesh size of about 0.1 x 0.1 inch^2 was used in the useful aperture. The largest mesh size was ~ 0.25 x 0.25 inch^2 in the steel farthest from the aperture. The mesh plot for the B2 magnet is shown in Figure 1. This shows the conductor placement. cooling holes, insulation and pole shape. Figure 2 shows the flux lines for a central field of 15 kG.

The procedure was to adjust the coil spacing and pole shape to produce a uniform field for infinite permeable steel. When this was acceptable the field shapes for 15, 18, 21 and 22.5 kG (500 GeV) were calculated to show the saturation effect. This cycle was repeated until the normalized gradient k = (dB/dR)/B_o was less than .005/m over 90 percent of the aperture for fields up to 18 kG. In each case, the AMPFAC (ratio of required current for a given B relative to the infinite permeability case) was calculated. This is given in Table 1 for fields up to 22.5 kG. It is important to have the same AMPFAC for both magnets so that they can be powered in series by the same power supply.

Graphs of the calculated k versus x for the final design of the B1 and B2 magnets are given in Figures 5 and 6. In both magnets the curves meet the design requirement. A B-H table was used in the computer program, based on measurements made by the National Bureau of Standards on samples of the actual steel, but modified to agree with model measurements at high fields. This ignored the fact that the outer angle plates welded to the steel laminations are made of a slightly different steel. This effect was calculated and found to be negligible.

Pole Shape Design

Both square and tapered pole shapes were investigated in the early design studies.[2,3,4] The tapered pole shape was adopted for the final design because a wider good field is attained at high fields. For a given radial position, the value of k increases with field from 18 to 22.5 kG for the square pole shape. For the tapered and shimmed pole, the value of k increases with field from 18 to 20 kG, then decreases from 20 to21.5 kG and then increases again from 21.5 to 22.5 kG. Hence, the variation in k is less at higher fields with the tapered poles.

For the same yoke thickness, the tapered pole has an AMPFAC 2 percent smaller at 18 kG and 7 percent smaller at 22.5 kG than the square pole. Thus, electric power is saved with the tapered pole.

To make the good magnetic field region as wide as possible, positive and negative shims are used, as shown in Figs. 3 and 4. With these shims the good field region was extended about 0.2 to 0.3 inch on both sides. The good field regions are 4.7 and 3.7 inches wide for the B1 and B2 magnets respectively for fields up to 18 kG. These small shims slightly complicate the work of making the dies. The tolerance of points on the pole face of the laminations was ± 0.2 mil.

Tolerances on the Coil Geometry

The position of the inner conductors between the top and bottom pole faces is very critical to the shape of the magnetic field inside the gap. These effects were calculated with a small computer program, and the optimum position was found.

The tolerance on the conductor position was calculated with TRIM for infinite permeable steel. The results are given in Figs. 7 and 8 and show that the inner conductors should be placed with a tolerance of ± 5 mils.

The position of the water cooling holes relative to the verticle dimensions of the conductor is also important. The position of the hole along the length of conductor was measured and found to be within tolerance.

Vacuum Chamber

The rectangular vacuum chambers used in the bending magnets are made of 205 stainless steel tube of 50 mil thickness. The permeability of 205 stainless steel is about 1.002 at 200 Oe. The effect of the chamber was calculated with TRIM and causes a small negative sextupole term due to the shape of the chamber. The effect on k is less than -0.002 at 1.5 inch for a B2 magnet. A welded seam along the length of the vacuum chamber increases the local permeability. Therefore, the vacuum chamber was made with the seam on the side and near the conductors. One chamber was made of stainless steel 304 which has a higher permeability so the effects were quite noticeable.

Magnet End

The inner coil is bent either upwards or downwards at the end due to the special structure of the coil. This causes an asymmetry in the magnetic field at the end. To correct for this effect the bending magnets were installed to alternate with up-bent coils and down-bent coils.

Stamping Dies

Three dies for each of the B1 and B2 bending magnets have been used to punch roughly four million laminations of each magnets. They were made of high carbon high chrome steel instead of carbide steel due to shorter delivery time. The punched laminations from each die were inspected every month or so, and after each resharpening. On the average they were sharpened every three months.

The dies were made with an accuracy of ± 1 mil for the outside dimensions of the cores, and the pole face areas were made with an accuracy of ± 0.1 mil. It is important to keep the pole surface parallel to the bottom line of the back legs to within 0.2 mil over 5 inches, which introduces an error in k of 0.002/m. Deviations larger than this indicated a need to resharpen the die. The variation in the half-gap height of the lamination was within ± 0.5 mil, which corresponds to a change of ± 0.05% in B. Some measurements on the pole surface of the laminations showed variations of ± 0.2 mil occurring every quarter to half inch. About one-half of the bottom area of the sheared surface showed breaks due to punching. These effects seemed to cancel out statistically. The first set of B1 and B2 magnet dies were divided at the center of the pole pieces, which caused a step of 0.5 mil in the worst case on the pole surface of some laminations. The laminations were not punched in stages as is sometimes done to avoid warpage. Therefore, it was observed that occasionally the bottom line of the back legs was distorted up to 1.5 mil over 5 inches.

During stacking every three inches of laminations were flipped to average out any effects of punching deviations such as the effect of tapered laminations. Also, laminations from different dies were mixed to make half cores. This process averages out the first order error in the dies. Originally laminations with small irregu-

larities were sorted out; however, they amounted to only a few percent of the total number. Even these ended up in the magnets, in time, due to a shortage of laminations.

To check the effect of dies, several special magnets were made, in which the top and bottom laminations were punched from the same die and arranged to be a mirror image relative to the median plane. The measured gradient distributions are shown in Fig. 9. For this measurement, search coils and integrators were used with an automatic measuring table, and a Varian 6201 computer system to collect the data.[15]

Main Ring Magnet Steel

Since the bending magnets were intended to be powered up to 22.5 kG, the magnet should be capable of going to high fields with only a small saturation effect. The injection field is about 350 G for 7.2 GeV, requiring the steel to be as free as possible from the effects of nonuniform remanent fields. Therefore, the magnet steel should have a high μ-value at high fields and a small coercive force. Moreover, the cost was an important factor and paying a premium for special steel was to be avoided.

The whole order of magnet steel of about 10,000 tons for the main ring magnets including the bending and quadrupole magnets, was made at ARMCO Steel Company over a period of one year, starting in March, 1970. Steel was made in rolls of double width, and during processing was slit to the final width to reduce crown, then it was flattened and cut into sheets of about 10 feet by 25 inches.

The steel was made using conventional melting techniques resulting in ladle analysis similar to SAE 1008 steel but received special processing to fully decarburize the steel and develop a large grain size. Cold reduction of the product was used to produce a smooth surface providing a maximum space factor. The resulting steel has essentially non-directional magnetic characteristics.

Production Test for Steel

The sampling tests were done at NAL and ARMCO independently for every batch of about 50 tons. At NAL the following tests were performed:

1. Epstein Test. Samples 25 cm long were measured at 400 Oe using a home-made Epstein frame. The coercive force was measured as well as the μ-value at 400 Oe. The samples were cut parallel and perpendicular to the rolling direction and mixed in each arm of the Epstein frame.
2. Insulation Test. Sixteen pieces of the above samples were stacked and pressed in a home-made special press at 300 psi. A dc current of 1A was applied through the stack, and the insulation was calculated from the resulting voltage. The steel has a phosphate coating of Class C-4. The minimum resistance was set at 30 milliohm-cm^2 for 300 psi.
3. Space Factor Test. The volume of the sample was measured under pressure using the same press and the space factor was calculated by measuring the weight. The space factor was always greater than 0.98 for these as sheared samples.
4. Crown Test. This was made on samples which were cut across the width of about 25 inches. Eight pieces were stacked in the same direction and the total thickness at two inch intervals was measured, thus obtaining the average crown over the total width. After re-stacking by reversing the top four pieces, the same measurement was performed to check tapering. The resultant effective crown per lamination was less than 0.5 mil.

At ARMCO Steel Company, the Epstein test was performed at 10 Oe to measure the coercive force, similar measurements on the insulation test and crown test were carried out, and the Rockwell hardness test with limits of 20 to 40 was performed.

The data taken at NAL was averaged over a heat of about 200 tons. Individual and averaged data over a heat were used as the criteria for acceptance of the steel. The results of measurements at both places were usually in agreement. About 5% of the total steel was rejected due to excessive coercive force or crown. The distributions of the coercive force at 10 Oe, μ-value at 400 Oe, crown and space factor are shown in Figures 10, 11, 12 and 13.

The incoming steel sheets were divided into two groups of high and low coercive force. During assembly of a core these two groups were mixed half and half to reduce the variation of remanent field.

Production Magnetic Measurements

Magnetic testing and measuring was performed on all magnets prior to installation in the accelerator tunnel. The basic measurements performed on each magnet determines the difference in magnetic length relative to a reference magnet at several excitations, corresponding to 9, 18, 21 and 22.5 kG. The homogeneity of the magnetic length for several positions across the gap is also measured. The remanent field is measured after exciting the magnet up to 22.5 kG.

These measurements are made by stretching a two turn loop of 0.002 inch tungsten wire through the magnet. The spacing of the wire loop is 1 inch and is determined by quartz rods at each end. The loop is held in a fixture at each end of the magnet so that it can be radially translated or rotated in the magnet. For measuring the difference in the magnet length, the output voltage of this loop is bucked against a coil rigidly imbedded in a reference magnet that is excited in series with the magnet under test. The resultant error voltage is integrated, amplified, ditigized and sent to a small computer for analysis and comparison with a current and field signal.[15] Data are taken at settings slightly below and above the desired field and entered into the computer. By interpolating the data, the computer calculates the error for the desired field. The remanent field is measured by flipping the coil. This measurement is made after pulsing the magnet to full excitation several times to set the remanent field.

Periodic remeasurement of the same "standard" magnet was used to check the measuring system. Measurement of this magnet has shown the rms statistical error to be ± 0.02% for the magnetic length and ± 1.0 Gauss for the remanent field.

In order to increase the resolution, some "hand" measurements were made at the 200 GeV level of magnet excitation (9 kG). The measurements employed the same stretched wire probe bucked against the reference magnet as used for the production measurements. With the coil stationary, the field is lowered quickly from 9 kG to zero current, hence the measurements are D.C. but the remanent field effects are not included. The increase in resolution is obtained through precise control of the integrator drift at each data point.

The deviations for fourteen B1 and fifteen B2 magnets were then averaged at each value of x. The averages, which are listed in Table 2, indicate a slight increase in bending length on either side of center. The average errors in these data are approximately ± .003%.

Results of Production Measurements

Since the remanent field is critical to injection a strong attempt was made to maintain a consistently low coercive force. Figure 17 presents the changes in the remanent field and Figure 14 shows the variations of the coercive force over the time the magnets were produced. Both sets of data have been smoothed so that long term variations can be observed. Good agreement exists if the proper time correlation is made. The 1.5 Gauss increase observed in the remanent field is related to the increase in the coercive force. Figure 10 and Figure 15 present the distribution of the coercive force and remanent fields of both magnets. The width of the coercive force distribution accounts for the wide variation in the remanent fields.

The variation at 18 kG during production is shown in Figure 18. The variations are related to the permeability of the steel, the sharpness and quality of the die and most significantly to the tightness of the gap in the return legs of the magnet. A burr resulting from a dull die could keep the gap slightly open. For magnets with a tight return leg, a 2 mil shim could not be inserted anywhere along the length of the magnet. This test eventually became the requirement for constructing magnets. Magnets which have low readings from 9 to 22.5 kG typically have a large average gap in the return leg of as much as 5 mils. The distribution observed at 9, 21, and 22.5 kG are virtually identical to the 18 kG errors shown.

A histogram of the field errors for remanent, 9, 18, 21, and 22.5 kG is presented in Figure 15. The clear and shaded peaks represent the B1 and B2 magnets respectively. Table 3 gives the mean and standard deviation for each case shown in this figure. At 18 kG both types of magnets have essentially the same bending length. At 9 and 21 kG the B1 is weaker than the B2 by approximately 0.2%. At 22.5 kG where saturation effects become large the magnets differ by 0.9%.

During operation of the accelerator, many magnets have failed and have been reprocessed. In order to remove the coil, the magnet is heated to burn out the epoxy. Then the welds are removed and the half cores separated. A new coil is inserted and the magnet reassembled with the burned cores. By comparing the magnetic measurements made before and after burning any changes should become apparent. This comparison is shown in Figure 16. The mean remanent field hardly changed. The 9 and 18 kG fields decreased by .04 ± .02% and the 21 kG field decreased by .01 ± .02%. Epstein samples which were heated in the same oven showed no change in permeability and surface resistivity.

Data from the various mechanical and electrical measurements made on main ring magnets have been summarized periodically to provide an ongoing check of their quality of construction and electrical integrity. These compilations have helped to establish standards by which replacement magnets can be accepted or rejected for use in the main ring.

The acceptance criteria are shown in Table 4. The quantity $\int Bdl$ is determined during the

magnetic measurement test with the technique described previously. The average values of $\int Bdl$ were established from the distributions shown in Figure 15. The quantity called "twist" refers to the maximum angle by which any two sections of the magnet can be rotated from each other. The magnets are optically surveyed at nine locations (18 points) along the top surface. The "sag", more or less self-explanatory, is also determined from these data. The series inductance is measured using a commercial inductance bridge at 1 kHz and checks for turn to turn shorts.

Acknowledgements

The authors wish to extend their sincere thanks to the many colleagues for their consultation and assistance during this project.

References

1. "Design Report," National Accelerator Laboratory, p. (5-2) July, 1968.
2. R.J. Lari, L.C. Teng, "Computer Design of the Main Ring Bending Magnets". NAL Internal Report, TM-149, 1968.
3. R.J. Lari and L.C. Teng, "Field Design of the Main Ring Bending Magnets of the NAL 200 GeV Synchrotron", IEEE Trans. Nucl. Sci. 16, No. 3, p. 667, (1969).
4. B. McD. Bingham, "Design of Main Ring Bending Magnets for Improved High Field Performance," NAL Internal Report TM-194 (1969).
5. R. Yamada, E.C. Berrill, T.W. Hardek, R.S. Odwazny, "The Magnetic Field Measurements of Mark I Model Magnet". NAL Internal Report FN-110, (1968).
6. R. Yamada, "DC Field Measurements on No. 2 Model Magnet", NAL Internal Report TM-82, (1968).
7. E. Malamud, "Measurement and Calculation of Eddy Current Effects in the B2 Magnets," NAL Internal Report TM-177, (1969).
8. E. Malamud and C. Schmidt, "Sextupole Comparison of Bending Magnet Steels", NAL Internal Report TM-172 (1969).
9. R. Yamada, "Iron Evaluation Tests for Main Ring Magnet", NAL Internal Report TM-171, (1969).
10. H. Hinterberger and R. Sheldon, "NAL Main Ring Magnets", The Third International Conference on Magnet Technology, Hamburg, May, 1970, p. 490.
11. W. Hanson, et al., "NAL Main Ring Integrally Impregnated Magnets", this Conference.
12. H. Hinterberger, et al., "Bending Magnets of the NAL Main Accelerator", IEEE Trans. Nucl. Sci. 18, No. 3, p. 853 (1971).
13. H. Hinterberger, et al., "Quadrupole Magnets of the NAL Main Accelerator," IEEE Trans. Nucl. Sci. 18, No. 3, p. 857, (1971).
14. A.M. Winslow, UCRL-7784-T rev. (1965), and J.S. Colonias, UCRL-16959 (1965) and UCRL-17340 (1967).
15. H. Feng, et al., "Automatic Magnetic Measurements Facility for Synchrotron Magnets", Proceedings of the Third International Conference on Magnet Technology, Hamburg, May, 1970, p. 1453.

Table 1

The Calculated AMPFAC ($NI_{\mu}/NI_{\mu=\infty}$)

B(kG)	9	15	18	20	21	21.5	22.5
B1	1.002	1.003	1.020	1.057	1.083	1.103	1.173
B2	1.001	1.003	1.024	1.061	1.084	1.099	1.153

Table 2

Deviation of the Quantity $\int Bdl$ at 9 kG in Percent Across the Horizontal Apeture for the Main Ring Bending Magnets

Magnet x =	+1.5	+1.0	0.0	-1.0	-1.5
B1 (%)	+.001	+.002	0	0	+.001
B2 (%)	--	+.002	0	+.003	--

Table 3

Mean Error and Standard Deviation Of B1 and B2 Magnets

	B1		B2	
	Mean	Deviat.	Mean	Deviat.
Rem.	16.8 G	±1.4G	13.0G	±0.9G
9kG	-.087%	±.083%	+.087%	±.073%
18kG	+.005%	±.083%	-.005%	±.066%
21kG	-.12%	±.077%	+.12%	±.060%
22kG	-.44%	±.07%	+.44%	±.06%

Table 4

Criteria for Production Magnets

Magnet	Type Quality	Criteria
B1	$\int Bdl$ at 200 GeV	-.09±.13%
B1	Series Inductance at 1kHz	1.57±.09mH
B2	$\int Bdl$ at 200 GeV	+.09±.13%
B2	Series Inductance at 1kHz	2.55±.10mH
B1, B2	Twist	.5 mrad max.
B1, B2	Sag	±.010 inch

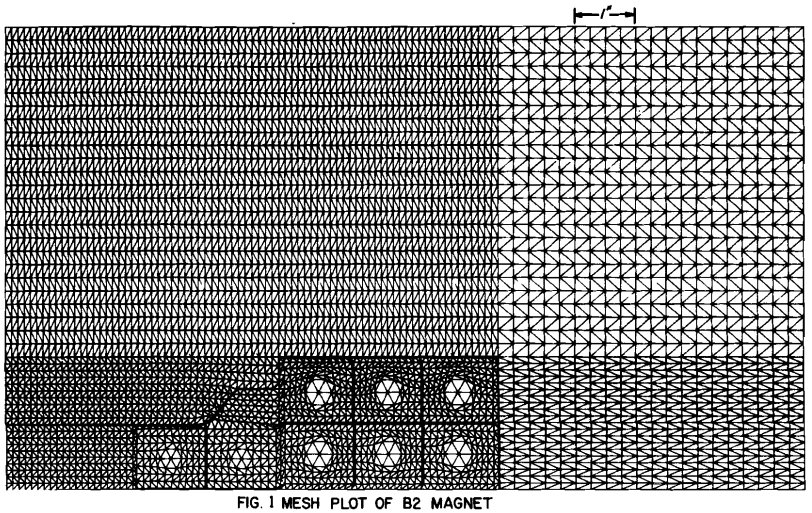

FIG. 1 MESH PLOT OF B2 MAGNET

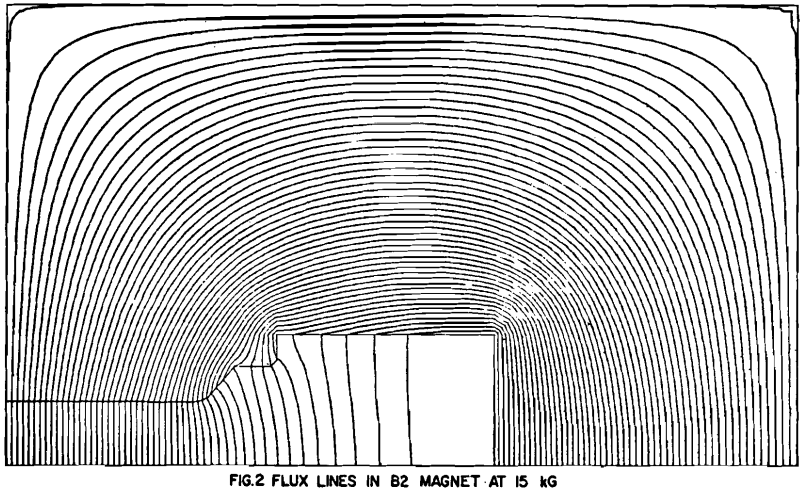

FIG.2 FLUX LINES IN B2 MAGNET AT 15 kG

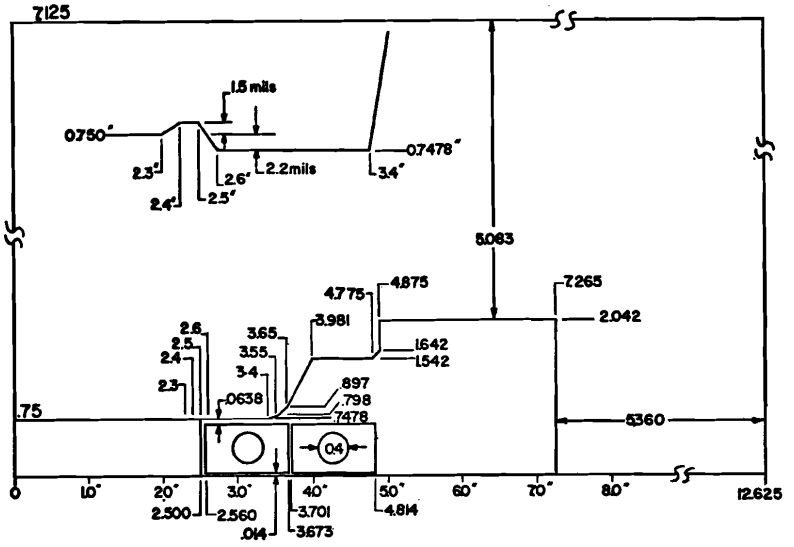

FIG.3 B1 POLE FACE DIMENSIONS

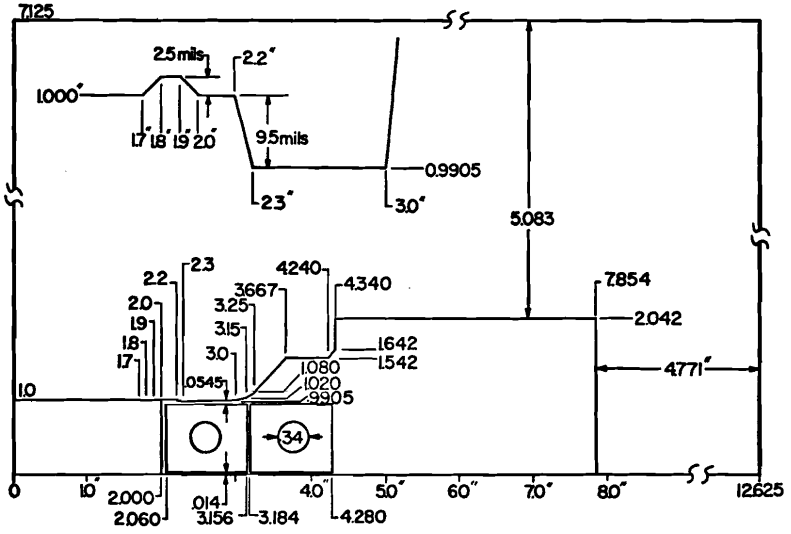

FIG.4 B2 POLE FACE DIMENSIONS

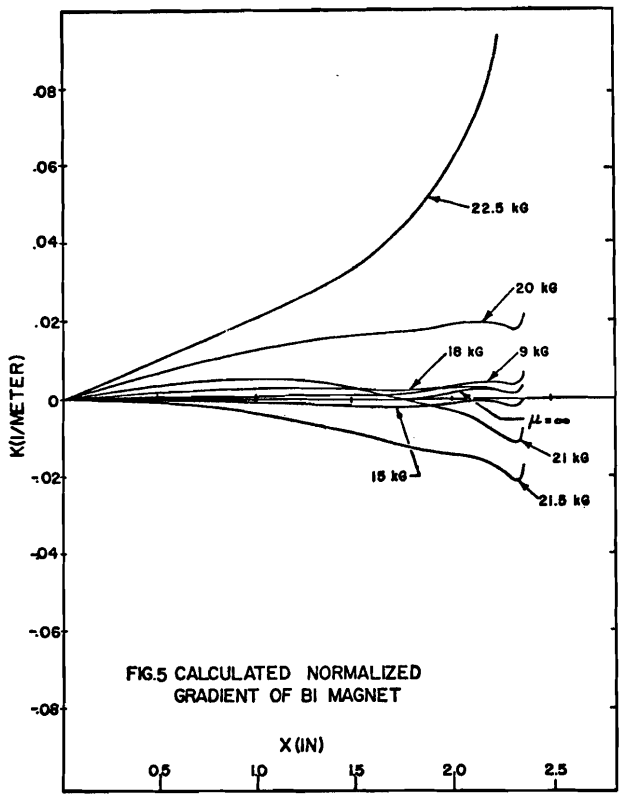

FIG.5 CALCULATED NORMALIZED GRADIENT OF B1 MAGNET

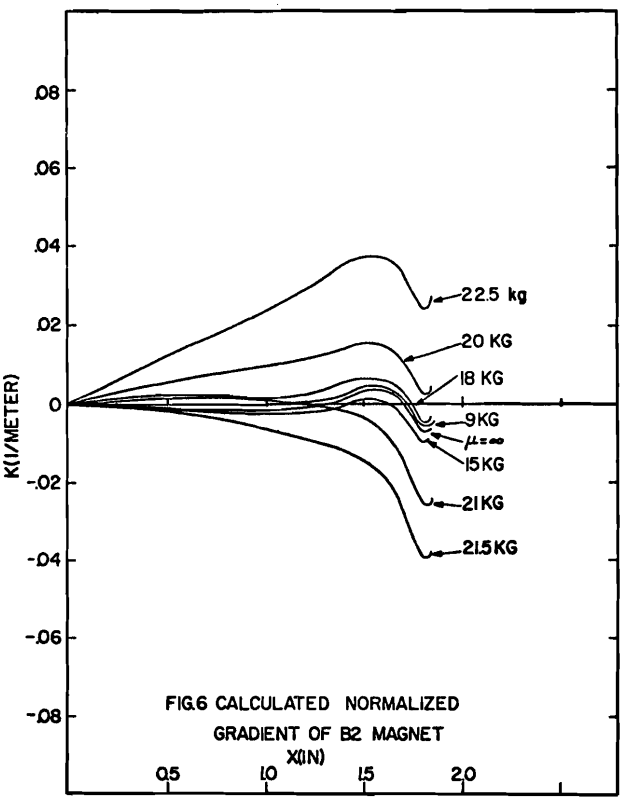

FIG.6 CALCULATED NORMALIZED GRADIENT OF B2 MAGNET

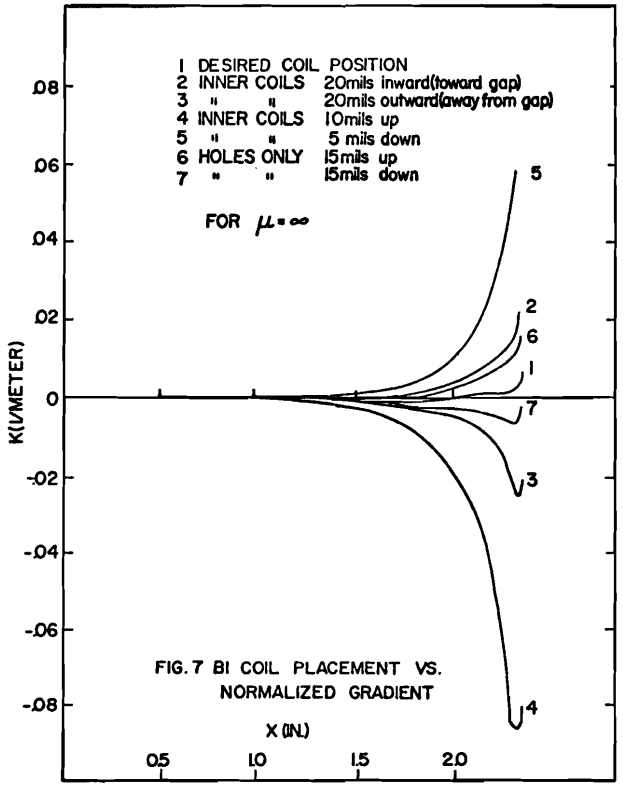

FIG. 7 B1 COIL PLACEMENT VS. NORMALIZED GRADIENT

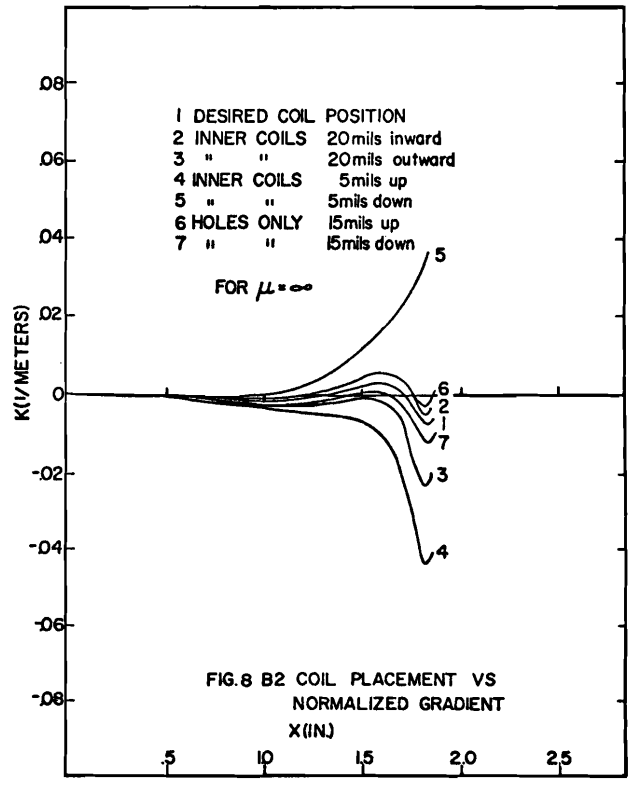

FIG.8 B2 COIL PLACEMENT VS NORMALIZED GRADIENT

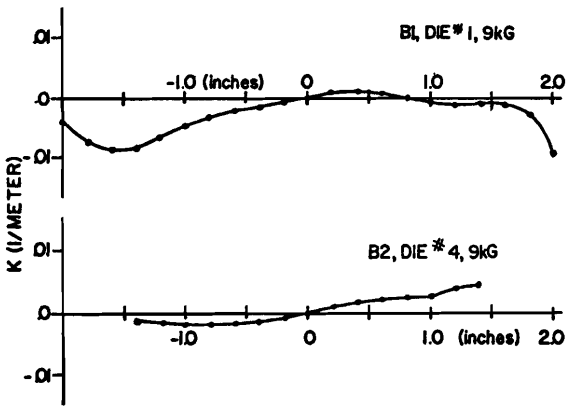

FIG.9 B1, B2, MEASURED NORMALIZED GRADIENT

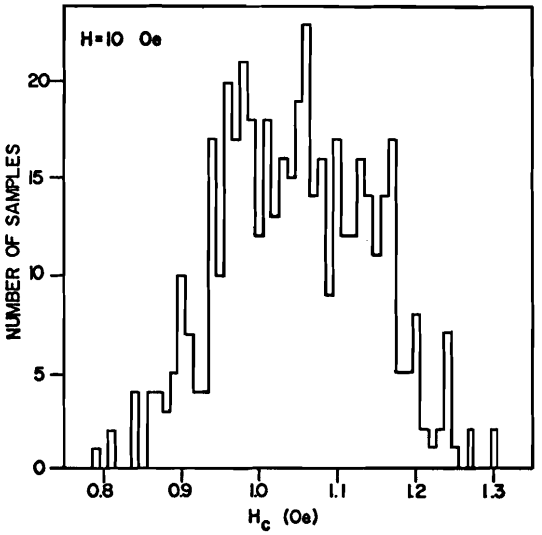

FIG.10 COERCIVE FORCE DISTRIBUTION

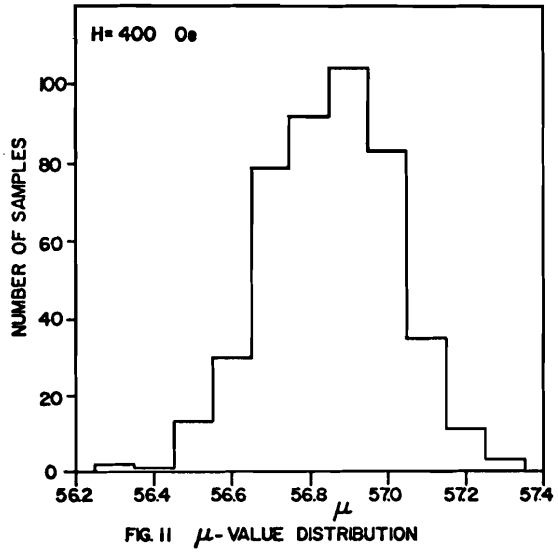

FIG. 11 μ- VALUE DISTRIBUTION

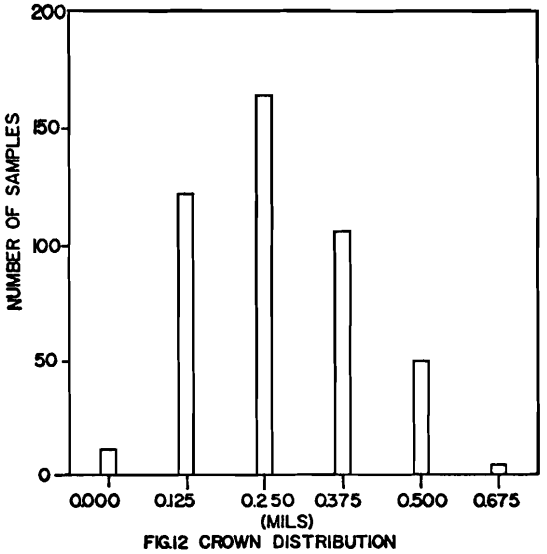

FIG.12 CROWN DISTRIBUTION

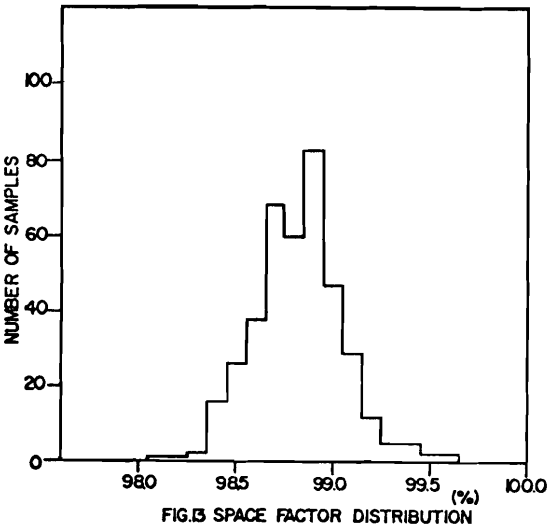

FIG.13 SPACE FACTOR DISTRIBUTION

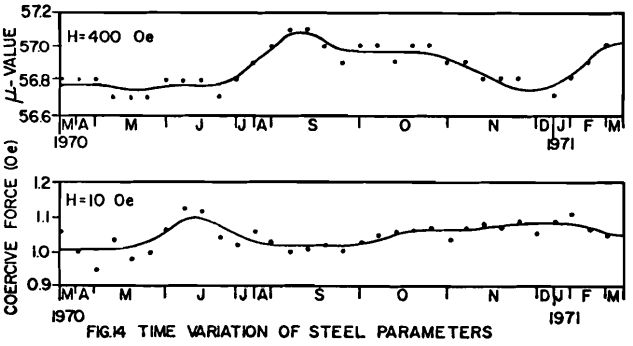

FIG.14 TIME VARIATION OF STEEL PARAMETERS

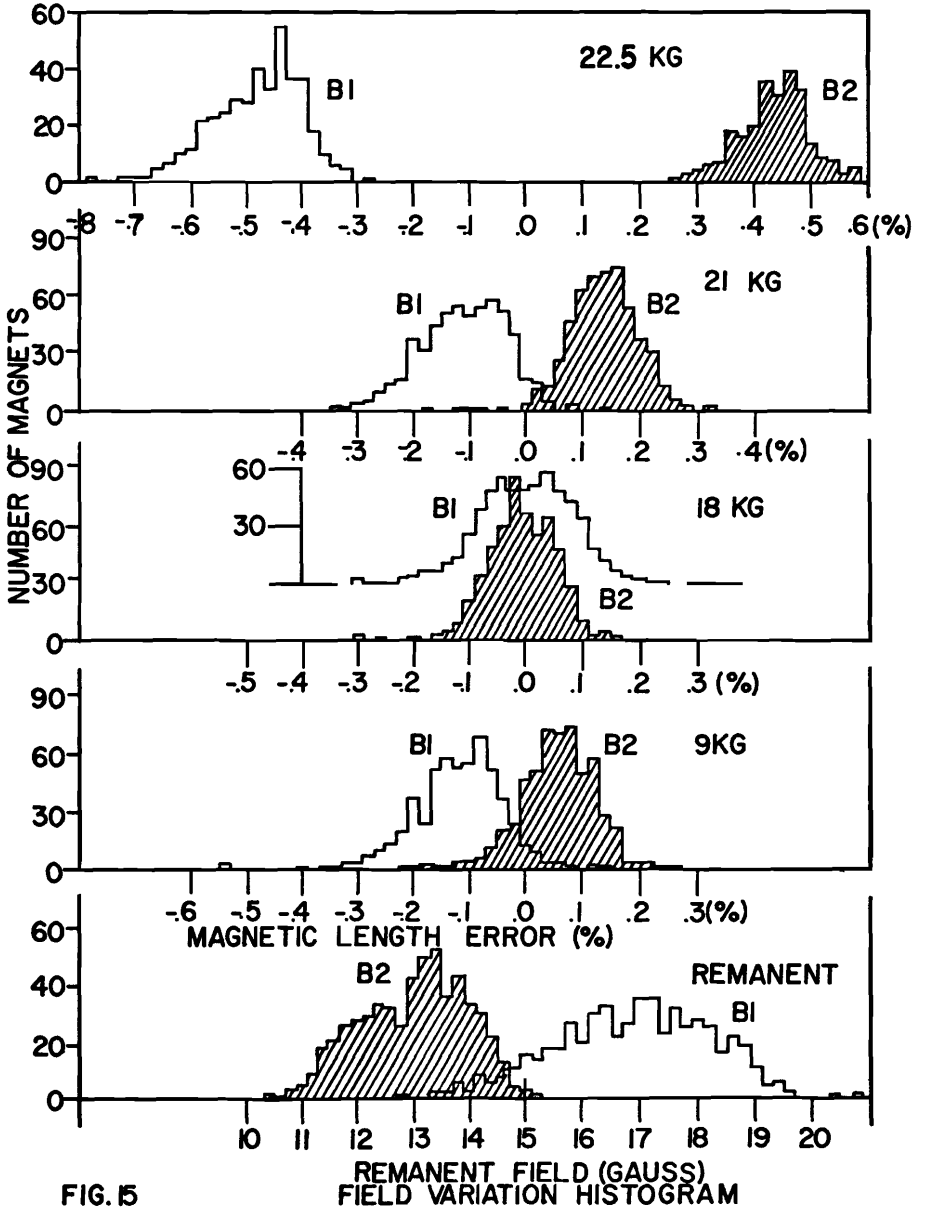

FIG. 15 FIELD VARIATION HISTOGRAM

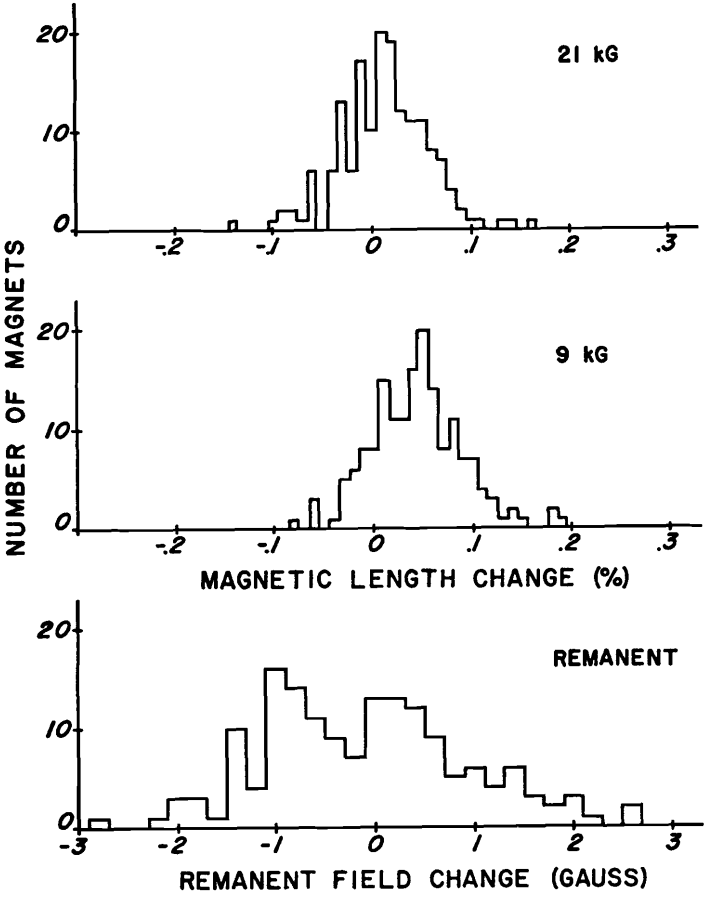

CHANGE IN FIELD AFTER REPROCESSING

Fig. 16

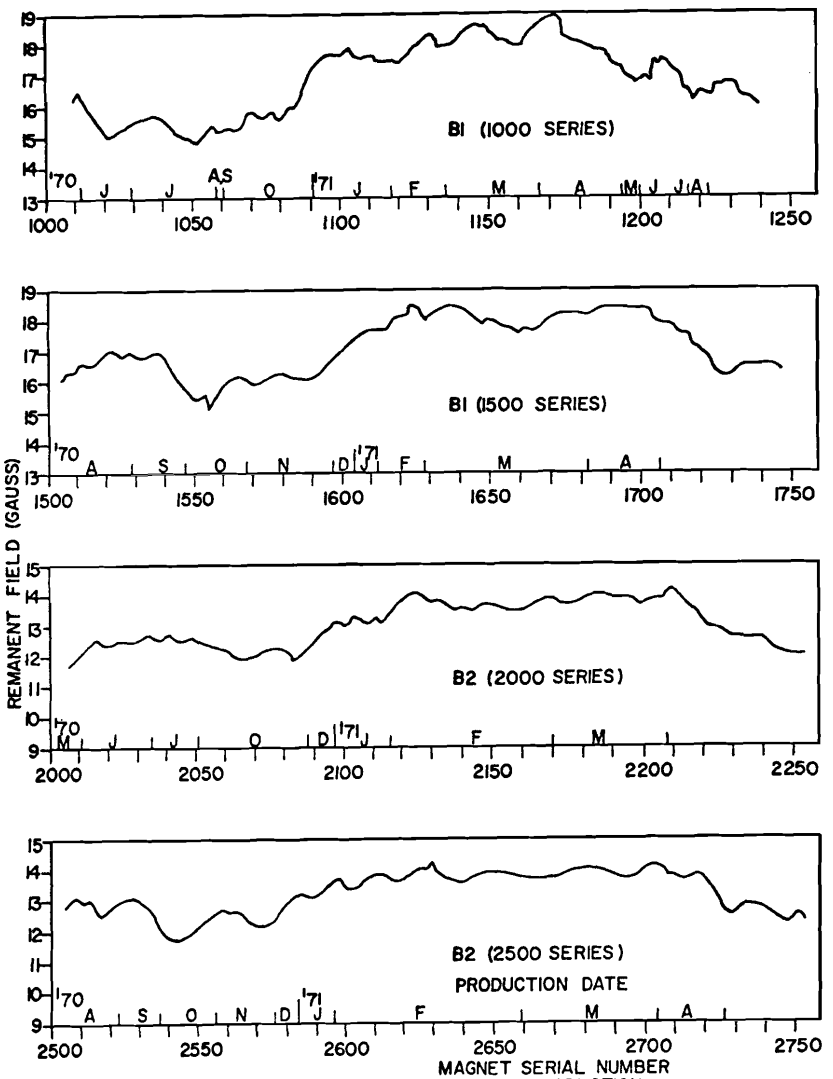

REMANENT FIELD VS. MAGNET PRODUCTION

FIG.17

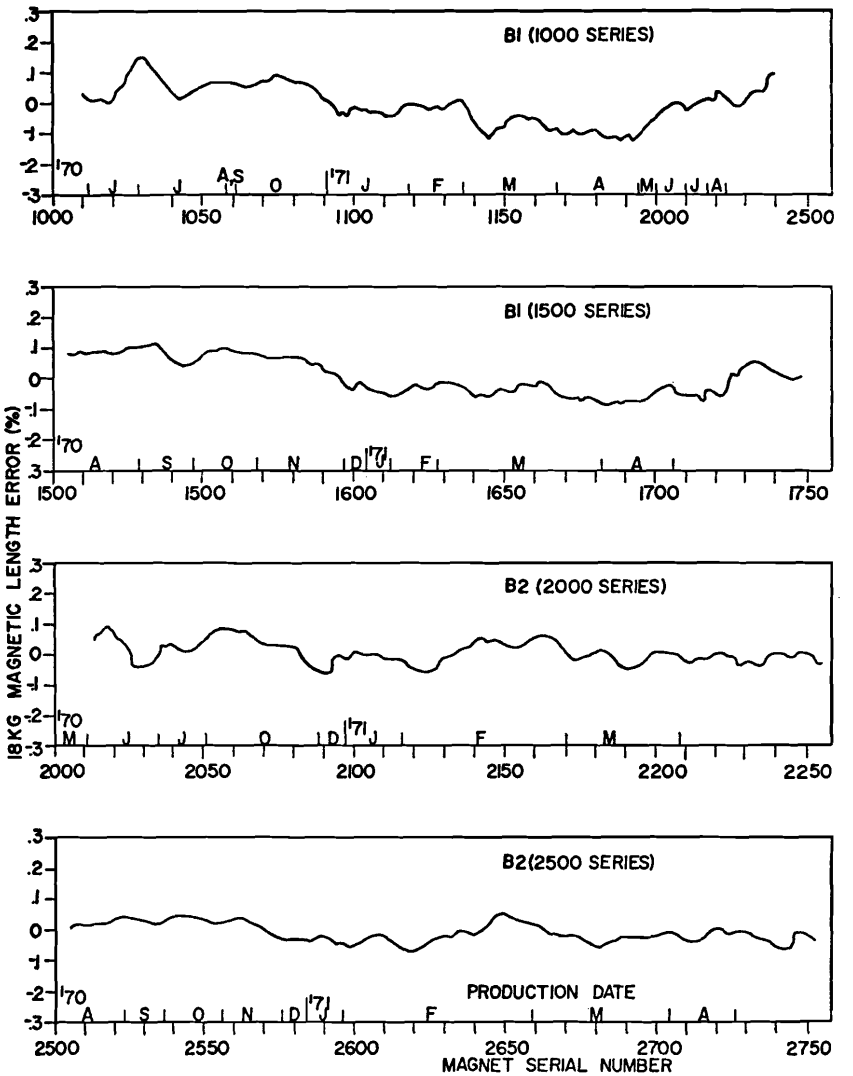

18 KG FIELD VS. MAGNET PRODUCTION

FIG. 18